

Chemical Science

Accepted Manuscript



This is an *Accepted Manuscript*, which has been through the Royal Society of Chemistry peer review process and has been accepted for publication.

Accepted Manuscripts are published online shortly after acceptance, before technical editing, formatting and proof reading. Using this free service, authors can make their results available to the community, in citable form, before we publish the edited article. We will replace this *Accepted Manuscript* with the edited and formatted *Advance Article* as soon as it is available.

You can find more information about *Accepted Manuscripts* in the [Information for Authors](#).

Please note that technical editing may introduce minor changes to the text and/or graphics, which may alter content. The journal's standard [Terms & Conditions](#) and the [Ethical guidelines](#) still apply. In no event shall the Royal Society of Chemistry be held responsible for any errors or omissions in this *Accepted Manuscript* or any consequences arising from the use of any information it contains.

COMMUNICATION

Ambient Condition Oxidation in Individual Liposomes Observed at the Single Molecule Level

Cite this: DOI: 10.1039/x0xx00000x

Robert Godin, Hsiao-Wei Liu and Gonzalo Cosa*

Received 00th January 2012,
Accepted 00th January 2012

DOI: 10.1039/x0xx00000x

www.rsc.org/chemicalscience

Single particle imaging studies on liposomes stained with lipophilic, fluorogenic, peroxy radical-trapping probes show oxidation taking place during standard liposome preparation conditions. A ratiometric assay involving the fluorogenic probe enables quantifying oxidative events at the single particle level. The assay provides a general strategy to monitor reactions on individual liposomes.

Free radical mediated lipid chain autoxidation of polyunsaturated fatty acids¹ (PUFA) is a prevalent chemical process with diverse ramifications given the widespread distribution of lipids in nature and in man-made materials. PUFA peroxidation is associated not only with a range of pathologies²⁻⁴ but also cellular signaling.⁵⁻⁸ It is further directly involved in food quality decay,⁹ and has the potential to impart structural alterations in lipid based products and materials such as biosensors, medical nano-devices for e.g. imaging, and liposome formulations for e.g. personal care or drug delivery.

The kinetics of lipid chain autoxidation and the effects of lipophilic antioxidants within the nano-confined boundaries of lipid membranes and lipid nanoparticles has attracted enormous attention over the years.¹ Liposomes have been the system of choice to study PUFA chain autoxidation and to better understand the antioxidant properties of various lipophilic compounds,¹⁰ in particular α -tocopherol, the most active naturally occurring lipid soluble antioxidant.¹¹ Liposomes have been additionally sought after as surrogate models of peroxidation in low density lipoproteins, small ca. 20 nm diameter lipid nanoparticles with a non-polar lipid core and a polar lipid shell.¹²

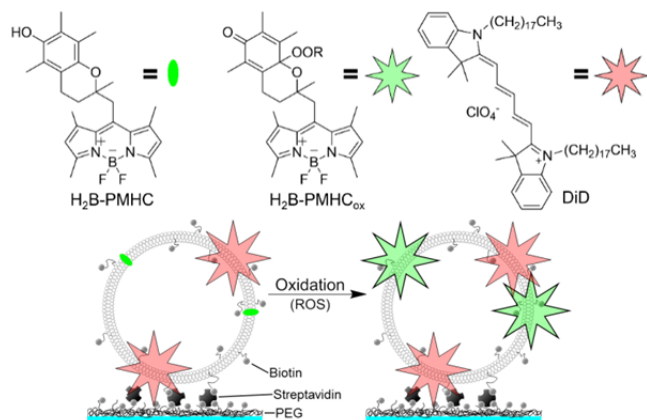
Here we report our ability to visualize the oxidation of single fluorogenic α -tocopherol analogues (trap-reporter probes that mimic the peroxy radical-scavenging activity of α -tocopherol¹³⁻¹⁸) embedded within the lipid membrane of surface immobilized liposomes at the

single molecule level (see Scheme 1). The tremendous sensitivity provided by our single molecule/particle assay shows that oxidative chemical events take place in individual liposomes under ambient conditions in the absence of additives intended as a source of reactive oxygen species (ROS). Our assay underscores the possible occurrence of lipid degradation taking place under standard liposome preparation conditions. It may also provide new approaches to decipher reaction mechanisms in a lipid membrane given its physical-chemical heterogeneity as a reaction medium. In general the assay further provides a simple sensitive way to monitor single chemical reactions¹⁹⁻²¹ at the level of individual liposomes.

Scheme 1 illustrates the experimental strategy used. The sample consisted of 100 nm diameter liposomes prepared from 1,2-dioleoyl-*sn*-glycero-3-phosphocholine (DOPC) (75,000 DOPC lipids/liposome on average).²² The liposomal membrane contained the fluorogenic α -tocopherol analogue H₂B-PMHC (ca. 100 molecules per liposome, i.e., 0.13 mol% vs. DOPC). Following scavenging of peroxy or alkoxy radicals with rate constants akin to those of α -tocopherol,¹¹ oxidized emissive H₂B-PMHC (H₂B-PMHC_{ox})¹⁵ is generated and the emission intensity undergoes a ca. 30 fold enhancement in liposomes upon deactivation of an intramolecular photoinduced electron transfer quenching pathway.¹³⁻¹⁷ The liposomes also contained the red-emitting lipophilic dye DiD (ca. 200 molecules per liposome, 0.27 mol% vs. DOPC). We utilized DiD as an orthogonal emissive dye to independently label and identify single surface anchored liposomes²³ before ABAP was flowed and H₂B-PMHC_{ox} was generated (see Figure 1).⁵ The dual labeling strategy further enabled ratiometric analysis (see below).

In order to anchor the liposomes on PEG-coated glass coverslips *via* biotin-streptavidin interactions, liposome formulations included 1 mol% vs. DOPC of 1,2-dipalmitoyl-*sn*-glycero-3-phosphoethanolamine-N-(biotinyl) (biotin-DPPE).²³⁻²⁶ Glass coverslips assembled with

SCHEME 1. EXPERIMENTAL STRATEGY.



a flow chamber were mounted on a piezoelectric nanopositioner. A confocal microscope was utilized to image the samples, where the green ($H_2B\text{-PMHC}$) and red (DiD) emissions were simultaneously collected in two parallel channels with two avalanche photodiode detectors. This setup provides optimum signal-to-background ratio. The circularly polarized 514 nm output of a CW Ar^+ laser was utilized to simultaneously excite the $H_2B\text{-PMHC}$ dye near its absorption maximum and the DiD dye at the blue edge of its absorption spectrum (see Figure S1).

We initially explored highly oxidative conditions in order to establish whether $H_2B\text{-PMHC}$ can report oxidation events in individual liposomes. Aqueous solution of the azo initiator 2,2'-azobis(2-amidinopropane) (ABAP, 0.25 M) in aerated phosphate buffered saline (PBS) were flowed over surface immobilized liposomes. ABAP thermally decomposes into 2 positively charged carbon centered radicals that upon reaction with oxygen yield 2 peroxy radicals (see Scheme S1). The rate of generation of these peroxy radicals is estimated to be $3 \times 10^{-8} Ms^{-1}$ at 23°C under our conditions.[‡]

Figure 1 displays images of the green channel recorded before (A) and during (C) flowing of ABAP. A 6-fold emission enhancement was recorded when comparing the total fluorescence intensity of all liposomes ($n = 159$) in the $H_2B\text{-PMHC}$ emission channel from images acquired before and during flow of ABAP solution (see also Figures S2 to S4). A 1.4 fold increase in the red channel was also recorded as ABAP was introduced, that we assign to energy transfer from emissive $H_2B\text{-PMHC}_{ox}$ to DiD . An increase in energy transfer was also observed in ensemble experiments upon oxidation of $H_2B\text{-PMHC}$. A ca. 3-fold increase in the background of the green channel was also observed throughout the image arising from impurities introduced with ABAP. Comparison of Figures 1A and 1C reveals that not all liposomes were observable in the $H_2B\text{-PMHC}$ channel before oxidative conditions. Thus, on a per liposome basis, a large range of enhancements was detected.

The dual labeling scheme incorporating DiD as an internal standard enabled us to quantify the change in $H_2B\text{-PMHC}$ fluorescence intensity in a ratiometric analysis that minimizes the influence of liposomal size distribution.^{11, 23, 27} DiD incorporation further enable us to account for all liposomes in the sample, even those not showing initial $H_2B\text{-PMHC}$ intensity. Figures 1E and 1F display the

observed linear correlation of the green ($H_2B\text{-PMHC}$) vs. the red (DiD) fluorescence intensity, recorded for each liposome before and after

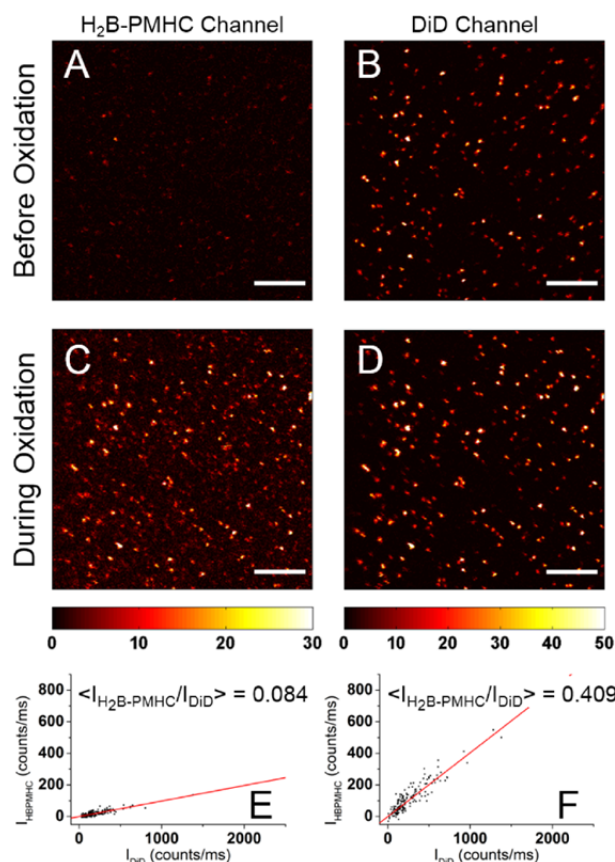


Figure 1. Fluorescence intensity images (top and middle rows) and intensity ratios of $H_2B\text{-PMHC}/DiD$ channels (bottom row) before and during oxidation initiated by ABAP. Panels A (C) show images corresponding to the $H_2B\text{-PMHC}$ channel and panels B (D) show those from the DiD channel, acquired before (during) oxidation, upon excitation with the 514 nm, 300 W/cm^2 output of an Ar^+ laser. Scale bars are 6 μm . Panels E (before oxidation) and F (during oxidation) illustrate the correlation of $H_2B\text{-PMHC}$ vs. DiD fluorescence intensity; also shown are linear fits as a guideline. Mean values of fluorescence intensity ratios obtained by Gaussian analyses are further listed.

ABAP addition, respectively. The larger slope for the latter illustrates the fluorescence enhancement caused upon peroxy radical reactions with $H_2B\text{-PMHC}$ on individual liposomes.

For a quantitative treatment we resorted to the distribution of the $H_2B\text{-PMHC}/DiD$ fluorescence intensity ratios. This treatment is less sensitive to outliers in comparison to a linear fit of the correlation of green to red intensity (Figures S5 and S6).^{27, 28} Histograms of intensity ratios were compiled for all liposomes in a $30 \times 30 \mu m^2$ area and fit to a Gaussian distribution. The mean value of the distribution was taken as the representative $H_2B\text{-PMHC}/DiD$ fluorescence intensity ratio of the sample (see Figure S4). We observed a maximal 4.9-fold fluorescence enhancement during oxidation. After longer exposure to oxidative conditions, fluorescence intensities in both $H_2B\text{-PMHC}$ and DiD channels decreased, consistent with oxidative degradation of the sample.¹⁵

Fluorescence enhancements of ca. 30-fold are typically recorded under thermal ABAP-initiated oxidation conditions executed in

ensemble experiments.¹⁵ Presumably, under our imaging conditions the adduct of H₂B-PMHC_{ox} and a positively charged peroxy radical resulting from ABAP decomposition may readily escape the liposome

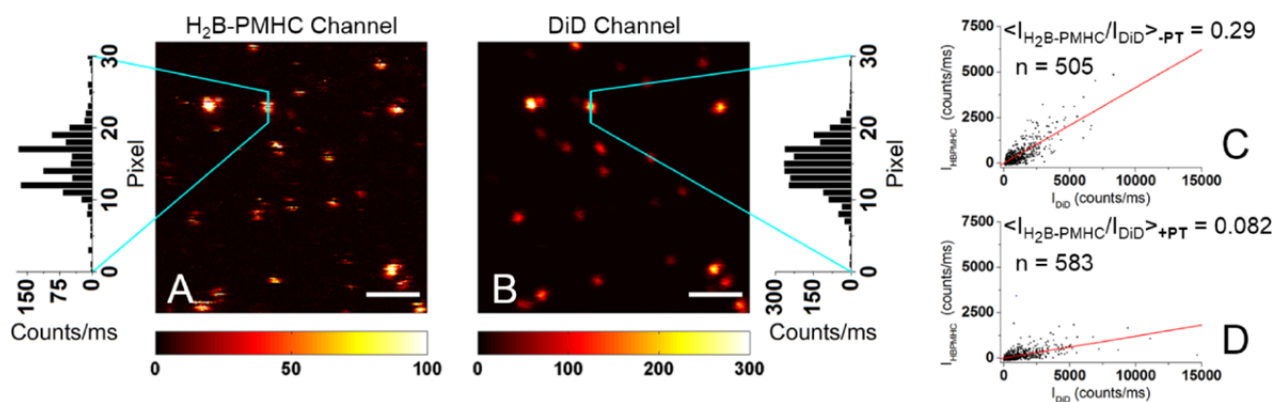


Figure 2. Panels A and B show fluorescence intensity images corresponding respectively to the H₂B-PMHC channel and the DiD channel, obtained for a sample prepared without Trolox and PMHC antioxidants (-PT). Images were simultaneously acquired using the 514 nm output of an Ar⁺ laser (6,400 W/cm²). Linescan profiles are shown at the sides of the images. Scale bars are 2 μm. Panels C (-PT) and D (+PT) illustrate the correlation of H₂B-PMHC vs. DiD fluorescence intensity in the absence and presence of antioxidants; also shown are linear fits as a guideline. Mean values of fluorescence intensity ratios, obtained by Gaussian analyses of data from 30 × 30 μm² images, are further listed.

during the image acquisition and diffuse away from the confocal observation volume. This is supported by confocal microscopy experiments that reveal that oxidation of H₂B-PMHC by lipophilic alkoxy radicals (generated from dicumyl peroxide) yield a more lipophilic product (5-fold larger H₂B-PMHC/DiD intensity ratio) than the one formed upon ABAP-initiated oxidation. FRET from H₂B-PMHC_{ox} to DiD and photobleaching of H₂B-PMHC_{ox} during imaging (albeit low excitation powers of 300 W/cm² were used) may also explain the smaller enhancement. Probe degradation upon oxidation of the BODIPY core is additionally expected from the high ABAP concentrations used. These conditions are needed in order to observe the H₂B-PMHC fluorescence intensity enhancement under short (5-10 minutes) monitoring periods.¹¹

We were initially surprised to see bright emission from single molecules in some of the “pristine” liposomes prior to ABAP addition, arguably the result of oxidative events during sample preparation. This prompted us to investigate the extent of ambient oxidation during standard liposome preparation in the absence of additives intended as a source of ROS (Figure 2). Four different sample preparations with different antioxidant loads were monitored utilizing the H₂B-PMHC/DiD fluorescence intensity ratio as a marker of ambient oxidation. Two samples contained either the lipophilic antioxidant 2,2,5,7,8-pentamethyl-6-hydroxy-chromanol (PMHC) (+P) or the hydrophilic antioxidant 6-hydroxy-2,5,7,8-tetramethyl-chroman-2-carboxylic acid (Trolox) (+T). Two more samples were also studied with no antioxidant (-PT), and with both antioxidants (+PT) included in the preparation. Given the stronger laser powers used (6,400 W/cm²) to facilitate the acquisition of intensity-time trajectories (see below) DOPC liposomes were prepared with a reduced load of DiD molecules (50, 0.07 mol%). Imaging was always performed under HEPES buffer flow with no added Trolox in order to isolate sample preparation effects.

Based on the images we obtained with the above samples, we concluded that there is significant, quantifiable fluorogenic probe oxidation occurring during typical liposome sample preparation in

ambient conditions. This is reflected by the 3.5-fold higher H₂B-PMHC/DiD fluorescence intensity ratio in the sample lacking any antioxidant (-PT) compared to the sample with both PMHC and Trolox (+PT) (Figure 2, panels C and D). The observed intensity ratio for our samples in increasing order was +PT ≲ +T ≪ +P ≲ -PT (Figures S7, S8 and Table S1). Under our conditions, Trolox clearly has a more potent protective antioxidant effect than PMHC. This could indicate that species responsible for ambient oxidation in liposomes originate within the water phase.

The alternative to probe oxidation occurring during liposome preparation (described in the above paragraph) is that preoxidized H₂B-PMHC existing as a trace contaminant in e.g. the dye batch was incorporated during the liposome preparation. Our experiments with antioxidants rule out this possibility, as neither Trolox nor PMHC may reduce preoxidized H₂B-PMHC_{ox} (Figure S9). The activity of these antioxidants is thus preventive, arising from trapping ROS in solution, rather than “curative” or healing.

Importantly, a control experiment described in Figure S10 shows that the potential photosensitization of ROS by DiD is not a prevalent phenomenon under our imaging conditions but may be observed under exhaustive irradiation conditions (Figure S11). Accordingly, the contribution of photogenerated ROS to the observed intensity enhancement of H₂B-PMHC is negligible.

We note that the unrivalled sensitivity of single molecule spectroscopy plays a major factor in enabling us to measure the small differences in fluorescence intensities under different antioxidant loading. Importantly, given the similar antioxidant activity of H₂B-PMHC and α-tocopherol,^{15, 29} our observations would imply that there is a significant degradation of antioxidant during sample preparation. This would have detrimental effects in the lifetime of lipid based products and materials enriched with α-tocopherol as a protective agent. The degradation of protective α-tocopherol in lipid formulations in turn underscores the potential lipid degradation under ambient conditions.

Close inspection of confocal images recorded under ambient condition showed fluctuations in the liposome intensity over time in the green channel, manifested as pixelated rather than smooth profiles as observed in the DiD channel. The difference in intensity profiles between both channels may be better appreciated from the image linescans for $10 \times 10 \mu\text{m}^2$ regions in Figure 2 (see also Figure S9). The highly dynamic green emission profile arises from fluctuations in the amount of emissive $\text{H}_2\text{B-PMHC}_{\text{ox}}$ with time in an individual liposome as the sample is raster scanned resulting in a distorted Gaussian shape. Overlaid in Figure 3 are the fluorescence intensity-time trajectories recorded on individual liposomes, without (-PT, Figure 3A) and with (+PT, Figure 3B) PMHC and Trolox. The fluorescence time trajectories highlight the on-off "blinking" of the $\text{H}_2\text{B-PMHC}$ probe (ca. 100 molecules/liposome). Conversely, the emission intensity arising upon DiD illumination (ca. 50 molecules/liposome) follows an exponential decay due to photobleaching, with a lifetime of approx. 10 s under our aerated imaging conditions. In the former case, the measured intensity counts per second recorded for $\text{H}_2\text{B-PMHC}_{\text{ox}}$ are those expected to arise from zero to a few dyes simultaneously emitting. In the case of DiD, the low excitation probability due to its small cross section at 514 nm results in a comparable intensity when all dyes in a liposome are emissive.

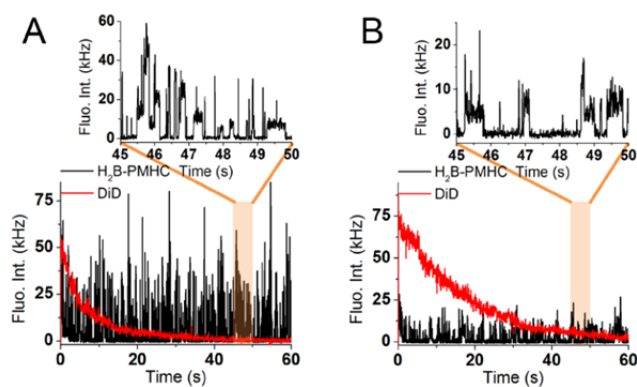


Figure 3. Intensity-time trajectories recorded for individual liposomes prepared (A) without (-PT) and (B) with PMHC and Trolox (+PT). The black and red traces correspond to the emission from the $\text{H}_2\text{B-PMHC}$ channel and the DiD channel. The data is binned at 5 ms. DiD traces are plotted every 10^{th} point for clarity.

While tempting to postulate that the emission dynamics are the result of the generation of $\text{H}_2\text{B-PMHC}_{\text{ox}}$ and its subsequent photobleaching, we may not currently preclude reversible photobleaching/blinking also operating on individual $\text{H}_2\text{B-PMHC}_{\text{ox}}$ molecules within the liposomes. A few hundreds of fluorescent bursts are observed within 3 minutes when focusing on liposomes, which is much greater than the average of 100 $\text{H}_2\text{B-PMHC}$ dyes per liposome. In contrast, typically less than 15 events are seen when looking at a region with no liposomes (see also Figure S12 and Table S1). Regardless of whether the dynamic emission profile results solely from reaction upon oxidation of the trap segment in $\text{H}_2\text{B-PMHC}$ or further involves photochemical/photophysical processes intrinsic to $\text{H}_2\text{B-PMHC}_{\text{ox}}$, it may prove uniquely powerful towards super resolution imaging of lipid substrates relying on stochastic processes.³⁰⁻³²

Conclusions

In summary, we have successfully detected reactions with peroxy radicals within individual liposomes utilizing the fluorogenic antioxidant probe $\text{H}_2\text{B-PMHC}$. The ratiometric assay we have developed has the sensitivity to observe oxidation events in individual liposomes under ambient conditions (typical laboratory temperature and lighting). These results stress the potential prominence of lipid degradation during their formulations. The new assay further provides a simple sensitive way to monitor chemical reactions at the level of individual liposomes. Our assay may become a powerful methodology towards studying oxidative phenomena taking place in nanoreactors such as liposomes and low density lipoproteins, as well as other systems of biological importance. We further believe that the emission dynamics may prove uniquely powerful towards super resolution imaging of lipid substrates.

Acknowledgements

G.C. is grateful to the Natural Sciences and Engineering Research Council (NSERC) and Canadian Foundation for Innovation (CFI) for funding. R.G. is thankful to NSERC for a postgraduate scholarship, H.-W.L. is thankful to the Drug Discovery and Training Program (CIHR) and GRASP (FRQS), for postdoctoral scholarships.

Notes and references

Department of Chemistry and Center for Self Assembled Chemical Structures (CSACS/CRMAA), McGill University, 801 Sherbrooke Street West, Montreal, QC, H3A 0B8, Canada. Email: gonzalo.cosa@mcgill.ca

† Electronic Supplementary Information (ESI) available: complete liposome preparation, single molecule setup and single molecule studies. See DOI: 10.1039/c000000x/

§ The spectroscopic properties of the dyes used combined with the emission filters employed in our setup (SI) gave rise to 7% $\text{H}_2\text{B-PMHC}$ to DiD channel crosstalk and negligible DiD to $\text{H}_2\text{B-PMHC}$ crosstalk.

‡ Calculated from its activation energy ($124 \text{ kJ} \cdot \text{mol}^{-1}$) and 10 hour half-life temperature (56°C).

¶ We note that by working with a single lipid rather than a mixture of lipids in the liposome formulation, the heterogeneities in dye concentration reported to occur with lipid mixtures, are expected to be minimal. The number of fluorescent dyes are a true marker of individual liposome size, and inhomogeneities in dye distribution, if any, will not introduce a systematic bias in liposome size determination. See reference 27.

¶¶ These conditions were chosen to limit the number of confocal images needed to observe the maximal fluorescence intensity to 1 or 2 images, in an effort to minimize photobleaching of $\text{H}_2\text{B-PMHC}_{\text{ox}}$.

1. H. Yin, L. Xu and N. A. Porter, *Chem. Rev.*, 2011, **111**, 5944-5972.
2. K. J. Barnham, C. L. Masters and A. I. Bush, *Nat. Rev. Drug Discov.*, 2004, **3**, 205-214.
3. V. W. Bowry and K. U. Ingold, *Acc. Chem. Res.*, 1999, **32**, 27-34.
4. V. E. Kagan, J. P. Fabisiak, A. A. Shvedova, Y. Y. Tyurina, V. A. Tyurin, N. F. Schor and K. Kawai, *FEBS Lett.*, 2000, **477**, 1-7.
5. F. J. Schopfer, C. Cipollina and B. A. Freeman, *Chem. Rev.*, 2011, **111**, 5997-6021.
6. R. West, C. Panagabko and J. Atkinson, *J. Org. Chem.*, 2010, **75**, 2883-2892.
7. C. C. Winterbourn, *Nat Chem Biol*, 2008, **4**, 278-286.

8. T. K. Rudolph and B. A. Freeman, *Sci. Signal.*, 2009, **2**, re7.
9. T. Waraho, D. J. McClements and E. A. Decker, *Trends Food Sci. Technol.*, 2011, **22**, 3-13.
10. E. Niki and N. Noguchi, *Acc. Chem. Res.*, 2003, **37**, 45-51.
11. G. W. Burton and K. U. Ingold, *Acc. Chem. Res.*, 1986, **19**, 194-201.
12. M. Alessi, T. Paul, J. C. Scaiano and K. U. Ingold, *J. Am. Chem. Soc.*, 2002, **124**, 6957-6965.
13. P. Oleynik, Y. Ishihara and G. Cosa, *J. Am. Chem. Soc.*, 2007, **129**, 1842-1843.
14. K. Krumova, P. Oleynik, P. Karam and G. Cosa, *J. Org. Chem.*, 2009, **74**, 3641-3651.
15. K. Krumova, S. Friedland and G. Cosa, *J. Am. Chem. Soc.*, 2012, **134**, 10102-10113.
16. K. Krumova and G. Cosa, *J. Am. Chem. Soc.*, 2010, **132**, 17560-17569.
17. A. Khatchadourian, K. Krumova, S. Boridy, A. T. Ngo, D. Maysinger and G. Cosa, *Biochemistry*, 2009, **48**, 5658-5668.
18. K. Krumova, L. E. Greene and G. Cosa, *J. Am. Chem. Soc.*, 2013, **135**, 17135-17143.
19. L. Zang, R. Liu, M. W. Holman, K. T. Nguyen and D. M. Adams, *J. Am. Chem. Soc.*, 2002, **124**, 10640-10641.
20. K. Naito, T. Tachikawa, M. Fujitsuka and T. Majima, *J. Phys. Chem. B*, 2005, **109**, 23138-23140.
21. T. Cordes and S. A. Blum, *Nature Chemistry*, 2013, **5**, 993-999.
22. V. P. Torchilin and V. Weissig, eds., *Liposomes*, Oxford University Press Inc. , NY, 2003.
23. A. T. Ngo, P. Karam, E. Fuller, M. Burger and G. Cosa, *J. Am. Chem. Soc.*, 2008, **130**, 457-459.
24. E. Boukobza, A. Sonnenfeld and G. Haran, *J. Phys. Chem. B*, 2001, **105**, 12165-12170.
25. I. Cisse, B. Okumus, C. Joo and T. Ha, *Proc. Natl. Acad. Sci. USA*, 2007, **104**, 12646-12650.
26. D. Stamou, C. Duschl, E. Delamarche and H. Vogel, *Angew. Chem. Int. Ed.*, 2003, **42**, 5580-5583.
27. J. Larsen, N. S. Hatzakis and D. Stamou, *J. Am. Chem. Soc.*, 2011, **133**, 10685-10687.
28. E. Elizondo, J. Larsen, N. S. Hatzakis, I. Cabrera, T. Bjørnholm, J. Veciana, D. Stamou and N. Ventosa, *J. Am. Chem. Soc.*, 2011, **134**, 1918-1921.
29. B. Li, J. R. Harjani, N. S. Cormier, H. Madarati, J. Atkinson, G. Cosa and D. A. Pratt, *J. Am. Chem. Soc.*, 2012, **135**, 1394-1405.
30. G. De Cremer, B. F. Sels, D. E. De Vos, J. Hofkens and M. B. J. Roeffaers, *Chem. Soc. Rev.*, 2010, **39**, 4703-4717.
31. M. J. Rust, M. Bates and X. Zhuang, *Nat Meth*, 2006, **3**, 793-796.
32. T. Tachikawa and T. Majima, *Langmuir*, 2012, **28**, 8933-8943.